Correlation between sphere distributions of gamma-ray bursts and CMB fluctuations

O. V. Verkhodanov[1,*], V. V. Sokolov[1], M. L. Khabibullina[1]

[1]*Special Astrophysical observatory, Nizhnij Arkhyz, Russia; * vo@sao.ru*

Abstract Distribution of gamma-ray bursts (GRBs) from catalogs of the BATSE and BeppoSAX space observatories relative to the cosmic microwave background (CMB) data by Planck space mission is studied. Three methods were applied for data analysis: (1) a histogram of CMB signal values in GRB directions, (2) mosaic correlation maps calculated for GRB locations and CMB distribution, (3) calculation of an average response in the area of "average GRB population" on the CMB map. A correlation between GRB locations and CMB fluctuations was detected which can be interpreted as systematic effects in the process of observations. Besides, in the averaged areas of CMB maps, a difference between the distributions of average fluctuations for short and long GRBs was detected which can be caused by different natures of these events.

Keywords: cosmic background radiation, gamma-ray bursts, statistics, data analysis

1. Introduction

The quality of sky surveys carried out in the recent decade in different wavelength ranges allows us to study matter distribution in the observable part of the Universe based on many observational effects. Apart from direct measurement of the parameters of galaxy distribution and reconstruction of the large scale structure, as was done in the SDSS survey [1], there are many effects enabling the restoration of matter distribution. Among them there are effects of the secondary CMB anisotropy: the integrated Sachs–Wolfe effect [2] caused by changes in the CMB photon frequency in the variable gravitational potential of forming galaxy clusters and prevailing on the scales greater than 10°, the Sunyaev–Zel'dovich effect [3] on the scales of less than 10°, arising in interactions between the hot electrons in galaxy clusters with the CMB photons (the inverse Compton effect), the effects of scattering during the reionization epoch, and simply obstructive factors in the form of microwave emission of radio sources and galaxy clusters. Gamma-ray bursts are also an independent sign of the Large Scale Structure (LSS) allowing us to trace matter distribution at cosmological distances. The observable uniform distribution of gamma-ray bursts projected on the celestial sphere as well as the distribution of the bulk of radio sources (except for the faintest ones related to the nearest galaxies) demonstrate the cosmological principle requiring the Universe to be uniform and isotropic irrespective of the observer's location [4]. The observations show that the size of the largest structures is of order of 400 Mpc [5]. On lower scales, especially at low redshifts ($z < 0.1$), the matter is distributed anisotropically and inhomogeneously. However, the search for large structures continues at $z<1$ too (see, e.g., [6, 7]). Note that integral and statistical characteristics of the CMB distribution determined from the correlation maps with the SDSS galaxy locations show the presence of certain isolated scales of 2–3° within the redshift range $z = 0.8–2$ which corresponds to the linear scale of 60 Mpc and can be interpreted as the maximum size of a heterogeneity cell [8 – 12]. This agrees with the model of radio source activity in the range of $z \sim 1–2$ [13, 14], where the gravitational potential variations in forming clusters are expected. In this respect the comparative distribution of the CMB map extrema and GRBs on the celestial sphere is interesting as a new indicator of the LSS signature on the CMB maps at different redshifts. The uniform observable distribution of GRBs also allows us to test the cosmological principle. Besides, it is assumed

that they can be used as standard candles for the estimation of distance to objects under consideration [15, 16]. The available rather large catalogs – namely, BeppoSAX1 (Satellite per Astronomia X, "Beppo" in honor of Guiseppe Occhialini) [17] and BATSE2 (Burst and Transient Source Experiment) [18], comprising such objects – allow us studying the spatial distribution of these objects.

In recent years many authors investigated the gamma-ray distribution using various methods [19 – 26]. Among this research, paper [23] can be marked, where authors studied GRBs of short ($t < 2$ s), medium ($2 < t < 10$ s), and long ($t > 10$ s) duration from the BATSE catalog by different methods (by means of the Voronoi tessellations, minimum spanning tree, and multifractal spectrum). For the first two groups they discovered deviations from homogeneity as compared with model data. On this basis they discuss the satisfiability of the cosmological principle. In paper [26], the locations of the supernova explosions with $z < 1.4$ and gamma-ray bursts were used as the probing objects. For the supernova data a deviation from the uniform distribution on the diagram "CMB temperature in a source direction – z" was discovered in contrast to the similar diagram for gamma-ray bursts. The authors explain this difference by the contribution of the integral Sachs–Wolfe effect.

Earlier [24, 25], we studied the statistical correlation properties of sky distribution of GRBs relative to CMB by the mosaic correlation mapping method [27, 28]. The study involved the WMAP3 (Wilkinson Microwave Anisotropy Probe) data [29], the data from the Italian-Dutch BeppoSAX satellite (the energy range 0.1–200 keV, 781 sources) and results of the BATSE experiment (20 keV – 2 MeV, 2037 sources). Each catalog was divided into two subsamples containing short (lasting $t < 2$ s) and long ($t > 2$ s) events. If we assume that GRBs are related to massive spiral (for long GRBs) or elliptic (for short bursts) galaxies and, respectively, their location is related to the large-scale structure, then one can study the statistics of CMB inhomogeneities arising due to effects of the secondary anisotropy. Thus, the GRB locations can be related to the distribution of CMB fluctuations (e.g., revealing themselves by deviations from the statistical anisotropy) in those celestial sphere regions where the GRBs were registered. Since in most cases the main problem when studying GRBs is a large size of error boxes determining the source coordinates (of about $1° \times 1°$), we worked with maps smoothed to $1°$. Our previous work with the WMAP data resulted in the discovery of a correlation between the CMB peaks and GRB locations which, in particular, can be caused by the systematic effects. The discovered correlation between the GRB locations and the CMB distribution is sensitive to the equatorial coordinate system and can be caused, for example, by the fact that the microwave radiation of the Earth gets to far side lobes of the power beam pattern.

Here, we applied and developed our approach for data of the Planck space mission [30], specifically, for the SMICA map [31]. Below we apply several statistical approaches to study the distribution of gamma-ray bursts on the sphere (see also details in [25]). Section 2 deals with the CMB signal statistics in the region of GRBs. Section 3 investigates the mosaic correlations of CMB maps (Planck SMICA) and GRB locations. Further (Section 4) we use the averaging procedure (stacking) of CMB map fields in the direction of a gamma-ray burst to estimate the average "population" microwave signal. The obtained results are discussed in Section 5.

2. Statistics of CMB Signal in Gamma–Ray Burst Regions

The SMICA CMB map [31] of the Planck experiment was restored from the multifrequency observations obtained with the High Frequency Instrument (HFI) at the 100, 143, 217, 353, 545, 857 GHz bands and with the Low Frequency Instrument (LFI) at 30, 44, 70 GHz. Resolution of the CMB map was about 5. In spite of the fact that the Planck mission is secondary with respect to another NASA space mission – WMAP (Wilkinson Microwave Anisotropy Probe), its observational characteristics are better. Among them one can mark out a higher resolution (by 3 times), which gave an opportunity to measure the angular power spectrum to higher harmonics (i.e., to higher values of l), a higher sensitivity

(by 10 times), and 9 frequency bands, improving the procedure of separation of the background components. These Planck parameters allowed us to obtain new, practically independent (of WMAP) observational data. In this paper we used the SMICA map smoothed to max = 150, and in a number of cases we applied the Mask-Ruler Minimal_2048_R1 mask [30]. To analyze the statistics of pixel values, we used the *mapcut* procedure of the GLESP package5 [32]. Calculations were made for the maps smoothed to the resolution of 260 (l_{max} = 20), 35 (l_{max} = 150), 20 (l_{max} = 300), and 10 (l_{max} = 600). Figure 1 shows the locations of GRBs from the subsamples of BeppoSAX and BATSE catalogs on CMB maps with the resolution 260' (l_{max} = 20). The map resolution was selected in accordance with the expected scale of the Sachs–Wolfe effect manifestations and possible appearance of some features on the SMICA map.

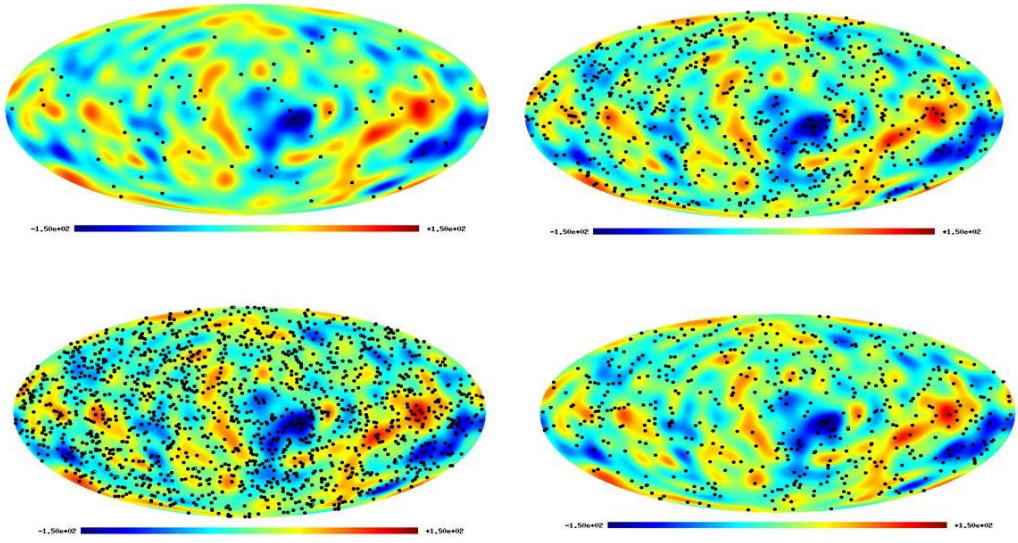

Fig1. *The location of GRBs from different samples on CMB maps with the resolution l_{max} = 20. The top left image shows the BeppoSAX data, t < 2 s. The top right image shows the BeppoSAX data,t > 2 s. The bottom left image presents the BATSE data, t < 2 s. The bottom right image is for the BATSE data, t > 2s.*

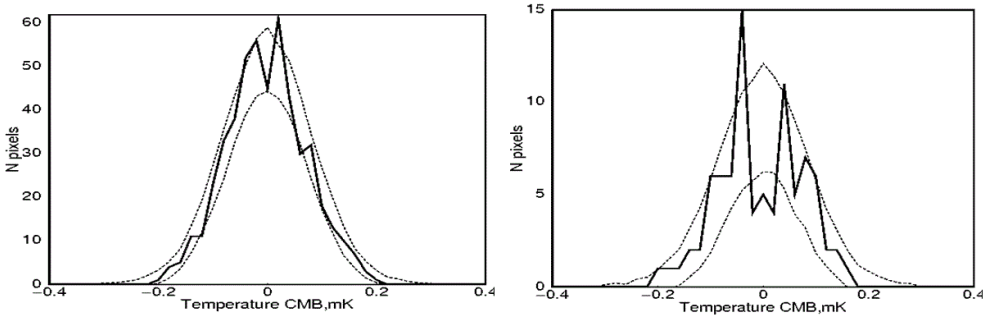

Fig2. *Distribution of CMB fluctuations in the SMICA map pixels corresponding to short (t<2s) GRB locations with the map resolution l_{max} = 150 for different GRB subsamples. The left diagrams show the distribution of short BATSE GRBs. The right picture gives the distribution of signals for short BeppoSAX GRBs. The dashed lines show the 1σ-dispersion of CMB values in the ΛCDM cosmological model calculated with 200 random gaussian realizations of the CMB signal.*

To search for potential correlations, we counted how many GRBs get into CMB pixels with negative values of signal fluctuations, which can be due to the above mentioned effects, on CMB maps with different resolutions. We calculated the statistics of CMB pixel values in the GRB locations for subsamples of BATSE and BeppoSAX catalogs for short and long events.

Figure 2 presents diagrams of distribution of the CMB fluctuation values for four subsamples of the GRBs and the CMB maps with different resolutions. The dashed lines show the expected 1σ-dispersion of CMB values in the ΛCDM cosmological model. Earlier [24], we discovered a deviation from what was expected with the Gaussian random CMB signal in the distribution of fluctuation values with the resolution l_{max} = 150 in regions of short BATSE GRBs. In the Planck data the deviations are also observed for short GRBs (see the left diagram in Fig. 2). Besides, there are small deviations from the models for long BATSE GRBs and short BeppoSAX GRBs at l_{max}=20 [25], short BeppoSAX GRBs at l_{max} = 150 (the right diagram in Fig. 2), long BATSE GRBs at l_{max} = 300, and long BeppoSAX GRBs at l_{max} = 600 [25]. To analyze the sphere distribution of those GRBs which are in the directions where the detected signal deviates from the expected one, we made pixelization with the *mappat* procedure from the GLESP software package [32]. The pixel size 700'x700' was chosen in such a way that the maximum pixel value (the number of events in a corresponding area) would not be less than 3 and a significant dynamic range for the harmonic analysis would be provided.

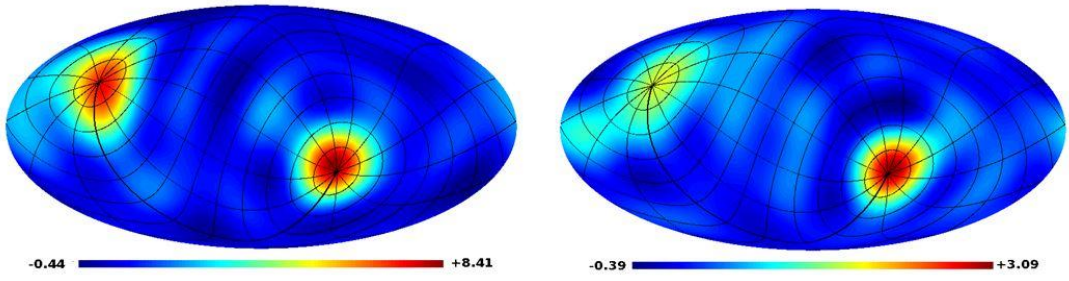

Fig3. *Examples of the smoothed maps of the sky up to l_{max} = 7 for different GRB subsamples The maps were built from the CMB pixels corresponding to the direction to those GRBs which deflect the histograms from the expected ones. The equatorial coordinate system was plotted on all maps. The left image presents data for GRBs compared with CMB in the maps with resolution l_{max} = 20 and long BATSE GRBs. The right plot demonstrates data of long BeppoSAX GRBs l_{max} = 600).*

Fig. 3 shows examples of the GRB maps pixelized and smoothed this way. Their contribution into the histogram exceeds the expected 1σ-dispersion. The equatorial coordinate system is plotted on all maps. All images demonstrate a nonuniform sphere distribution of events, concentrated near the equatorial poles. In many cases, the hot spots are located directly on the equatorial poles. In maps with l_{max} = 20 and l_{max} = 150 with short BeppoSAX GRBs, we observe clusterization of hot spots in the Galaxy plane, which is more noticeable on the octupoles of these maps (see all figures in [25]). In some cases, the presence or absence of events in the pole regions markedly points to the pole regions of the equatorial coordinate system. Note that the peculiarities of CMB data of the Planck mission are identical to those of WMAP data as compared with GRB locations. Namely, the deviations in the pixel statistics are related with signal in the GRB direction oriented in the equatorial coordinate system. In [24], we estimated the probability of getting the quadrupole minima into the regions of the 5° radius around the equatorial poles. To do that, we generated 10 000 random realizations of the Gaussian signal to pixelize GLESP with 102 pixels in the equator. The probability of random hits to the pole zone is 0.0035. For a more detailed study of the correlation effects, the mosaic correlation method, presented in paper [27], was applied here.

3. Correlation maps of Distribution of Gamm-Ray Bursts and Planck SMICA Data

To study the properties of maps of the GRB locations and CMB fluctuations, we have performed the mosaic correlation of "BATSE–CMB" maps with pixels of different sizes: 500'x500', 600'x600', and 900'x900', covering the areas within which the correlation factor was calculated. To do that, first we pixelized the maps of GRB locations in all four subsamples. As in the previous stage, the pixel size 200'x200' was chosen in such a way that the maximum value (the number of events in a corresponding area) would not be less than 3. The correlation results are shown in Fig. 4. To analyze the obtained result, we calculated the angular power spectrum (2) of the map using the spherical harmonics (multipoles) expansion of the signal distributed on the sphere (1):

$$\Delta S(\theta,\phi) = \sum_{\ell=1}^{\infty} \sum_{m=-\ell}^{m=\ell} a_{\ell m} Y_{\ell m}(\theta,\phi)\,, \tag{1}$$

$$C(\ell) = \frac{1}{2\ell+1}\left[|a_{\ell 0}|^2 + 2\sum_{m=1}^{\ell}|a_{\ell,m}|^2\right] \tag{2}$$

The angular power spectrum allows us to select the harmonics contributing to the correlation map. Figure 5 shows some examples of the power spectra of the correlation factor maps, calculated by the mosaic correlation method for the BATSE and CMB data. As is shown in Figs. 4, application of the mask retains location of local maxima in the power spectra of mosaic maps. In a number of cases, the application of the mask even amplifies the amplitude of an isolated harmonic. Figure 6 demonstrates examples of such harmonics. The fourth multipole of the mosaic correlation map with the window 500'x500' calculated for the BATSE data (t<2s) contains a feature – the coldest central spot in the galactic plane (Fig.6, left top). The quadrupole of the correlation map for the BATSE data (t>2s) with the window 900'x900' (Figure 6, left bottom) is sensitive to the equatorial coordinate system. Note that the

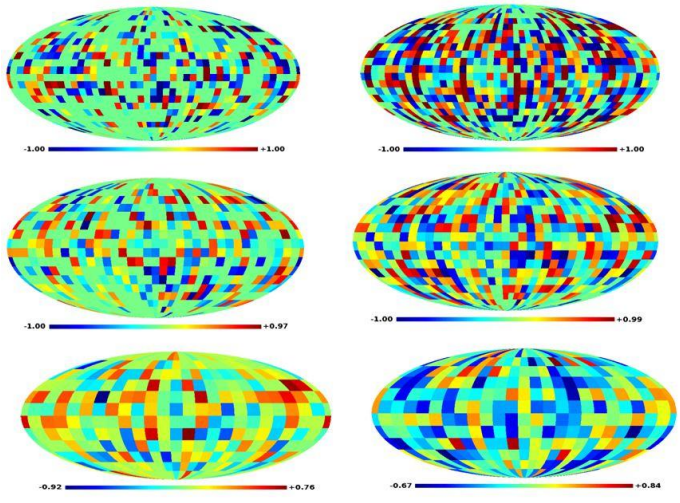

Fig4. *Correlation maps of CMB and BATSE GRB locations in the galactic coordinate system. The left column presents results of the CMB and BATSE (t < 2 s) data correlations, and the right one is for CMB and BATSE (t > 2 s). The upper pair of images demonstrates maps of l_{max} = 26 with the mosaic correlation pixel size w=500'x500'. The central pair shows the maps of l_{max} = 8 with the correlation pixel size w=600'x600'. The lower pair is for l_{max} = 5 and w=900'x900'.*

variation of the correlation scale (namely, the size of the area in which the correlation factor is calculated and attributed to a pixel of a mosaic map) changes the power spectrum. Thus, e.g., at a transition from the pixel side size of 500 to that of 600, the harmonic $l = 4$ amplitude in the power spectrum passes from the position of a local maximum to a local minimum. This can be caused by the increase in the amount of GRB events in the area of the corresponding size.

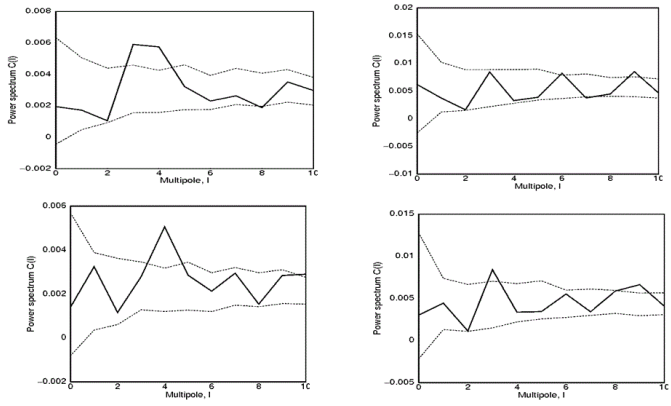

Fig5. *Power spectra of the correlation factor maps (with l_{max} = 26) calculated for the maps of BATSE GRB locations and CMB distribution (the solid line). The correlation pixel size is 500'x500'. The top left image shows the correlation spectrum of the BATSE data for t < 2s and CMB not accounting for the mask. The top right image contains the correlation spectrum of the BATSE data with t > 2s and CMB not accounting for the mask. The bottom left image demonstrates the correlation spectrum of the BATSE data for t < 2s and CMB accounting for the mask. The bottom right image shows the correlation spectrum of the BATSE data with t > 2s and CMB accounting for the mask. The images show the 1σ-dispersion obtained from results of analysis of 200 Gaussian random realizations of CMB.*

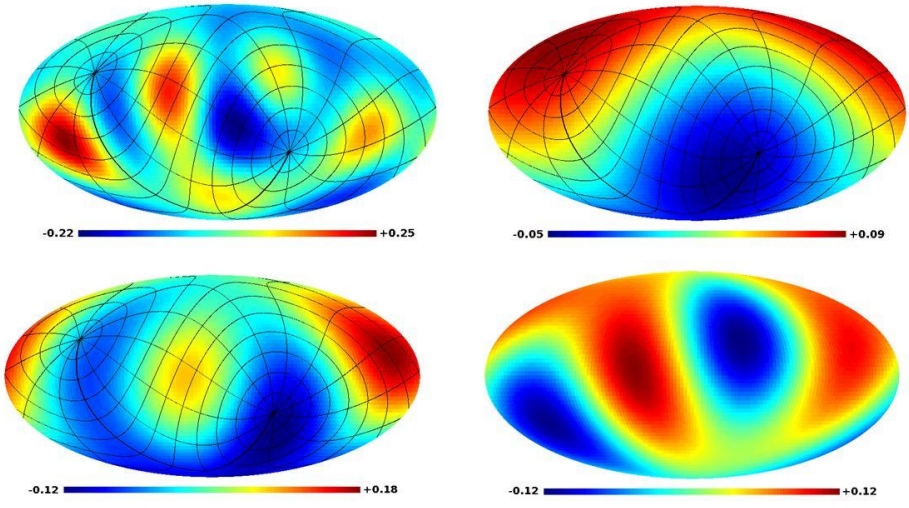

Fig6. *Maps of isolated harmonics in the power spectra. The images show the multipoles of mosaic correlations of the CMB and GRB locations. Top left: the isolated harmonics l=4 for the correlation window 500'x500' for BATSE data (t<2s); top right: the isolated harmonic l=1 for the correlation window 600×600. Bottom left: the correlation map for BATSE GRBs (t < 2s) and CMB with the correlation window 900'×900' (l= 2). Bottom right: the correlation map for the BATSE GRBs (t > 2s) and CMB with the correlation window 900'×900' (l= 2). Three maps contain the overlaid equatorial coordinate grid.*

4. Field Averaging

The Planck data allow us using the maps of a higher resolution than the WMAP archives. They can be used to estimate the potential signal from "an average population GRB" (the stacking procedure). To do that, areas of an identical linear or angular size around objects under investigation are selected in different directions on the celestial sphere. Then they are summed up to reveal an average signal. Because the redshift data are not available, we used the areas with identical angular sizes. To avoid the influence of a possible hard-to-consider signal of the Galaxy, we limited ourselves only to the regions around GRBs with galactic latitudes $|b| > 20°$. Among BATSE and BeppoSAX samples, this range includes 338 short (68% of the initial short BATSE GRBs) and 990 (64%) long events of the BATSE catalog, and 51 short (59%of the BeppoSAX list) and 454 (65%) long sources of the BeppoSAX catalog. For every GRB from our subsample, we have chosen a field in the Planck SMICA map of size 2°×2° in the tangential projection (the pixel size in the area is about 80″×80″). The selected areas were averaged. Results are shown in Fig. 7. Note that the addition of data from the region $|b| < 20°$ leads to the degradation (blurring) of images. The center of each averaged field in Fig. 7 gets into a local extremum region. Short BATSE and BeppoSAX GRBs are in the regions of background minima, and the long ones – in the regions of maxima. Ratios of the level of averaged fluctuation of the extremum into which a generalized GRB falls to the level of noise on the averaged maps are $dS/N = -1.65, 1.40, -1.43, 2.01$ for short and long BATSE GRBs and for short and long BeppoSAX GRBs respectively.

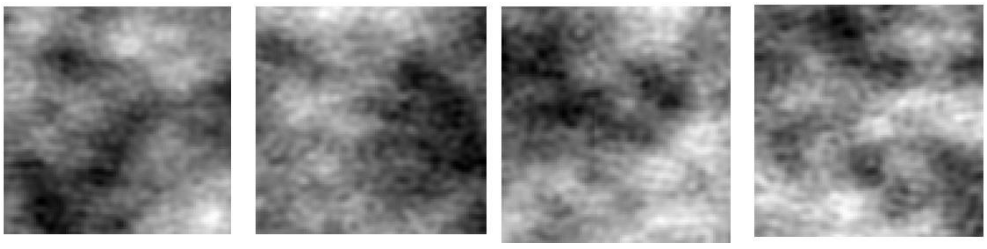

Fig7. *Results of the averaging of CMB fields, sized 2°×2°, in GRB directions. From left to right: fields of short BATSE GRBs; long BATSE GRBs; short and long BeppoSAX GRBs.*

5. Discussion

In this paper we investigated the CMB signal statistics in the direction of GRBs from the BATSE and BeppoSAX catalogs. The Planck SMICA map was used as the CMB map. We applied three approaches to study the properties of the GRB distribution on the sphere. They include: (1) the analysis of the Planck CMB signal value histogram in the direction to GRBs, (2) the study of mosaic maps built for GRB locations and CMB distribution, (3) the study of an average response on the CMB map in the region of the "average population GRB."

The application of the first two methods demonstrates that the correlation between GRB and CMB is caused, at least partially, by a signal in the equatorial coordinate system. This agrees with the results of our work [24, 25]. This relation can be caused by the modulation of the CMB signal observed in the L2 point by the microwave radiation of the Earth through the far antenna beam lobes. Deviations in distribution of GRBs towards the equatorial system are caused by non-uniform sky sensitivity (the time of signal accumulation) of the receiving equipment of the gamma-ray satellite observatories rotating around the Earth and always directed at the opposite side from it. Then an isolated character of the equatorial coordinate system naturally appears. Note that indication to the presence of signs of the equatorial coordinate system (e.g., location of spots) in the CMB data both for WMAP and Planck maps was already discussed in a number of papers [24, 25, 33, 34]. Besides, the radiation of the Earth can be

not a single factor. Another discussed reason can be the modulation of the solar wind by the Earth magnetic field passing through the point L2. It should be added that such effects, which are not detectable by the standard analysis, could be a source of the secondary Gaussianity observed at low harmonics [35 – 39]. The third method we have applied has shown that there is an insignificant difference at the level $|S/N| > 1.4$ which can randomly occur in less than 20% cases for the Gaussian noises in the distribution of the average CMB signal in GRB directions. As this takes place, short ($t < 2s$) GRBs in an averaged field gets to a local background minimum, and long $t > 2s$) GRBs – to a local maximum. If we assume that short GRBs occur in old elliptic galaxies formed from merging of less massive galaxies and located in the galaxy clusters, then a local minimum can be due to the Sunyaev–Zel'dovich effect [3]. The fact that long GRBs hit the local maximum in the CMB distribution could be caused by another effect. If long GRBs are related to supernova explosions, i.e., to star-forming galaxies, then even despite of location in a galaxy cluster, the proper microwave emission of a galaxy containing dust and gas would prevail over the effects of the surroundings and lead to appearance of a local maximum in the CMB maps. This effect could be tested by means of yet more sensitive data of the Planck experiment due to be published in the next release, expected in the second half of 2014.

Acknowledgements

The authors are grateful to EAS for the open access to the results of observations and processing of data in Planck Legacy Archive. For the analysis of extended emission on sphere we used the GLESP package [32, 40, 41]. M. L. Kh. and O. V. V. thank RFBR for a partial support of the project study by the RFBR grant No. 13-02-00027.

References

[1] D. J. Eisenstein, D. H. Weinberg, E. Agol, et al., Astron. J. 142 , 72, 2011.

[2] R. K. Sachs and A. M. Wolfe, Astrophys. J. 147, 73, 1967.

[3] R. A. Sunyaev and Ya. B. Zel'dovich, Astrophys. And Space Sci. 7, 3, 1970.

[4] P. J. E. Peebles, Principles of Physical Cosmology (Princeton Univ. Press, 1993).

[5] J. A. Peacock, Cosmological Physics (Cambridge Univ. Press, 2000).

[6] L. Rudnick, S. Brown, and L. R.Williams, Astrophys.J. 671, 40, 2007.

[7] V. Springel, C. S. Frenk, and S. D.M. White, Nature440 , 1137, 2006.

[8] J. Yadav, S. Bharadwaj, B. Pandey, and T. R. Seshadri,Monthly Notices Royal Astron. Soc. 364 , 601, 2005.

[9] P. Sarkar, J. Yadav, B. Pandey, and S. Bharadwaj, Monthly Notices Royal Astron. Soc. 399 , L128, 2009.

[10] F. Sylos Labini and Y. V. Baryshev, J. Cosmology and Astroparticle Phys. 6, 021, 2010.

[11] W. A.Watson, I. T. Iliev, J.M. Diego, et al., Monthly Notices Royal Astron. Soc. 437, 3776, 2014.

[12] Ya.V. Naiden and O.V. Verkhodanov, Astrophysical Bulletin 68, 471, 2013.

[13] J. F. Navarro, C. S. Frenk, and S. D. M. White, Astrophys. J. 490, 493, 1997.

[14] M. L. Khabibullina and O. V. Verkhodanov, Astronomy Reports 55, 302, 2011.

[15] L. Amati, F. Frontera; M. Tavani, et al., Astron. and Astrophys. 390, 81, 2002.

[16] L. Amati, C. Guidorzi, F. Frontera, et al., Monthly Notices Royal Astron. Soc. 391, 577, 2008.

[17] D. Riccia, F. Fioreb, and P. Giommia, Nuclear Phys. B Proc. Suppl. 69, 618, 1999.

[18] W. S. Paciesas, C. A.Meegan, G. N. Pendleton, et al., Astrophys. J. Suppl. 122, 465, 1999.

[19] R. Vavrek, et al., AIP Conf. Proc., No. 662, 163, 2003.

[20] L.L.R. Williams and N. Frey, Astrophys. J. 583, 594, 2003.

[21] A. Mészáros and J. Stocek, Astron. and Astrophys. 403, 443, 2003.

[22] A. Bernui, I.S. Ferreira, and C. A.Wuensche, Astrophys.J. 673, 968, 2008.

[23] A. Mészáros, L.G. Balázs, Z. Bagoly, and P. Veres, AIP Conf. Proc., No. 1133, 483, 2009.

[24] O.V. Verkhodanov, V.V. Sokolov, M.L. Khabibullina, and S.V. Karpov, Astrophysical Bulletin 65, 238, 2010.

[25] M.L. Khabibullina, O.V. Verkhodanov, and V.V. Sokolov, Astrophysical Bulletin 69, 472, 2014.

[26] V.N. Yershov, V.V. Orlov, and A.A. Raikov, Monthly Notices Royal Astron. Soc. 423, 2147, 2012.

[27] O.V. Verkhodanov, M.L. Khabibullina, and E.K. Majorova, Astrophysical Bulletin 64, 263, 2009.

[28] O.V. Verkhodanov and M.L. Khabibullina, Astrophysical Bulletin 65, 390, 2010.

[29] N. Jarosik, C.L. Bennett, J. Dunkley, et al., Astrophys. J. Suppl. 192, 14, 2011.

[30] P.A.R. Ade et al. (Planck Collab.), arXiv:1303.5062.

[31] P.A.R. Ade et al. (Planck Collab.), arXiv:1303.5072.

[32] A.G. Doroshkevich, O.V. Verkhodanov, P.D. Naselsky, et al., Int. J. Mod. Phys. D 20, 1053, 2011.

[33] O.V. Verkhodanov, Astrophysical Bulletin 69, 330, 2014.

[34] Ya.V. Naiden and O.V. Verkhodanov, Astrophysical Bulletin 69, 488, 2014.

[35] A. Rakic and D.J. Schwarz, Phys. Rev. D 75, 103002, 2007.

[36] Ja. Kim and P. Naselsky, Phys. Rev. D 82, 063002, 2010.

[37] O.V. Verkhodanov, Phys. Usp. 55, 1098, 2012.

[38] M. Hansen, J. Kim, A.M. Frejsel, et al., J. Cosmology and Astroparticle Phys. 10, 059, 2012.

[39] C.J. Copi, D. Huterer, D.J. Schwarz, and G.D. Starkman, arXiv:1311.4562.

[40] A.G. Doroshkevich, P.D. Naselsky, O.V. Verkhodanov, et al., Int. J.Mod. Phys. D 14, 275, 2003.

[41] O.V. Verkhodanov, A.G. Doroshkevich, P.D. Naselsky, et al., Bull. Spec. Astrophys. Obs. 58, 40, 2005.